

## Recent Forest Loss in the Brazilian Amazon Causes Substantial Reductions in Dry Season Precipitation

Yu Liu<sup>1,2</sup>, Dominick V. Spracklen<sup>2</sup>, Douglas J. Parker<sup>2,3</sup> , Joseph Holden<sup>4</sup> , Jun Ge<sup>1,5</sup> , and Weidong Guo<sup>1,5</sup> 

<sup>1</sup>School of Atmospheric Sciences, Nanjing University, Nanjing, China, <sup>2</sup>School of Earth and Environment, University of Leeds, Leeds, UK, <sup>3</sup>NORCE Norwegian Research Center, Bjerknes Center for Climate Research, Bergen, Norway, <sup>4</sup>School of Geography, University of Leeds, Leeds, UK, <sup>5</sup>Joint International Research Laboratory of Atmospheric and Earth System Sciences, Nanjing University, Nanjing, China

**Peer Review** The peer review history for this article is available as a PDF in the Supporting Information.

### Key Points:

- Recent forest loss (3.2%) in the Brazilian Amazon causes a mean 5.4% reduction in dry season precipitation
- 76.9% of reduced precipitation is due to decreased nonlocal water vapor, not local evapotranspiration
- Reduced convection and precipitation efficiency, caused by reduced moisture recycling, predominantly drive precipitation changes

### Supporting Information:

Supporting Information may be found in the online version of this article.

### Correspondence to:

W. Guo,  
[guowd@nju.edu.cn](mailto:guowd@nju.edu.cn)

### Citation:

Liu, Y., Spracklen, D. V., Parker, D. J., Holden, J., Ge, J., & Guo, W. (2025). Recent forest loss in the Brazilian Amazon causes substantial reductions in dry season precipitation. *AGU Advances*, 6, e2025AV001670. <https://doi.org/10.1029/2025AV001670>

Received 17 JAN 2025

Accepted 4 APR 2025

### Author Contributions:

**Conceptualization:** Dominick V. Spracklen

**Methodology:** Dominick V. Spracklen

**Supervision:** Dominick V. Spracklen, Douglas J. Parker, Joseph Holden, Jun Ge, Weidong Guo

**Writing – original draft:** Yu Liu

**Writing – review & editing:** Yu Liu, Dominick V. Spracklen, Douglas J. Parker, Joseph Holden, Jun Ge

© 2025. The Author(s).

This is an open access article under the terms of the [Creative Commons Attribution-NonCommercial-NoDerivs License](https://creativecommons.org/licenses/by/4.0/), which permits use and distribution in any medium, provided the original work is properly cited, the use is non-commercial and no modifications or adaptations are made.

**Abstract** The Amazon has experienced extensive deforestation in recent decades, causing substantial impacts on local and regional climate. However, the precipitation response to this recent forest cover change remains unclear. Here, we examined biophysical effects of forest cover change in the Brazilian Amazon on dry season precipitation using a regional coupled climate model with embedded water vapor tracers. We find that the 3.2% mean reduction in forest cover that occurred in Rondônia and Mato Grosso during 2002–2015 caused a  $3.5 \pm 0.8\%$  reduction in evapotranspiration and a  $5.4 \pm 4.4\%$  reduction in precipitation. The reduction in evapotranspiration warmed and dried the lower atmosphere reducing convection and precipitation. Reductions in incoming moisture, dominated by reduced moisture inflow in the mid-troposphere, accounted for 25% of the total reduction in moisture and amplified the precipitation response to forest loss. The reduction in precipitation efficiency explains 84.5% of the reduction in precipitation with the remainder due to reductions in precipitable water. The reduced precipitation sourced from water vapor inflow accounts for 76.9% of the simulated precipitation reduction, with the remaining 23.1% due to reduced local evapotranspiration. Our study demonstrates substantial reductions in dry season precipitation due to recent forest cover change in the Amazon, highlighting the importance of atmospheric responses to land cover change in this region.

**Plain Language Summary** In recent decades, the Amazon has experienced substantial deforestation. The loss of tropical forests has large impacts on the water cycle and can cause reductions in regional rainfall, with implications for the sustainability of neighboring forests and agriculture. Our study aimed to determine how recent deforestation in the Brazilian Amazon has affected rainfall in the region. We examined the impacts of observed forest cover change on precipitation in Rondônia and Mato Grosso during 2002–2015 using a water vapor tracer embedded in a regional coupled climate model. We show that forest loss of 3.2% reduced dry season precipitation by 5.4%, highlighting a high sensitivity of rainfall to land cover in the Amazon. Forest loss caused reductions in evapotranspiration that reduced convection and associated precipitation. In turn, these changes altered atmospheric circulation, which lowered the flow of atmospheric moisture sourced from outside of the region. Reductions in convection are the dominant cause of reduced precipitation, explaining 84.5% of the precipitation reduction in the dry season. Our study provides new insight into precipitation responses to forest cover change and the associated mechanisms in the Brazilian Amazon.

## 1. Introduction

The Amazon Basin is the world's largest tropical forest and most biodiverse terrestrial ecosystem (Jenkins et al., 2013). It plays a crucial role in regulating the Earth's climate (Artaxo et al., 2022) and provides diverse ecosystem services (Borma et al., 2022) but faces threats from deforestation, degradation, fire and climate change (Marengo et al., 2018). Deforestation affects regional climate (Lawrence et al., 2022), resulting in local (Alkama & Cescatti, 2016) and regional warming (Butt et al., 2023) and altered patterns of precipitation (Smith, Baker, & Spracklen et al., 2023; Smith, Robertson, et al., 2023) increasing exposure to heat stress (Alves de Oliveira et al., 2021) and reducing the productivity of forests (Li et al., 2022), agriculture (Leite-Filho et al., 2021) and hydropower (Stickler et al., 2013). However, the response of precipitation to forest cover change is highly uncertain; improved knowledge is crucial for informing forest protection and sustainable forest management (Ellison et al., 2017).

The Amazon basin experienced a rate of forest loss of  $\sim 27,000 \text{ km}^2 \cdot \text{yr}^{-1}$  during 2001–2016 (Qin et al., 2019), and about 17% of the Amazon basin had been deforested by 2021 (Science Panel for the Amazon, 2021). Rates of forest loss have been fastest in the southern Amazon, known as the “arc-of-deforestation.” The pattern of land cover change is complex with large areas of fast re-growing secondary forest from post-agricultural abandonment (Heinrich et al., 2021; Wang et al., 2020). Forest degradation from logging and fire as well as natural disturbances such as wind throw also impact large areas (Csillik et al., 2024). Global greening due to changes in climate and carbon dioxide concentrations, may be increasing leaf area index particularly in areas unaffected by land-use change (Piao et al., 2020). This complex pattern of land cover change contrasts with the simple representations that are used in many studies.

Vegetation plays a fundamental role in the entire hydrological cycle, and vegetation change can influence the terrestrial water balance through biophysical processes (Spracklen & Garcia-Carreras, 2015). Forest cover change alters surface albedo, aerodynamic roughness and evapotranspiration (Bright et al., 2017; Davin et al., 2007; Steyaert & Knox, 2008) which can all result in altered precipitation. Altered albedo and surface roughness can cause thermally- (Garcia-Carreras & Parker, 2011) and dynamically-driven (Khanna et al., 2017) atmospheric circulations that can initiate convection and alter patterns of precipitation. Recycling of evapotranspired moisture accounts for 24%–41% of the annual mean precipitation across the Amazon basin (Baker & Spracklen, 2022) and up to 48% in the state of Rondônia (Mu et al., 2021). There is also evidence that evapotranspiration helps initiate convection, particularly during the dry–wet season transition period (Wright et al., 2017). Deforestation in the Amazon during the past few decades has caused observed reductions in rainfall (Smith, Baker, & Spracklen et al., 2023; Smith, Robertson, et al., 2023) as well as shortening and delaying the onset of the rainy season (Leite-Filho et al., 2019).

Numerous regional and global climate modeling studies of Amazon deforestation have been conducted in the last few decades, but the simulated impacts of land cover change on precipitation are still highly uncertain. A synthesis of model studies found that large-scale deforestation of the Amazon Basin would reduce precipitation by  $12\% \pm 11\%$  (Spracklen & Garcia-Carreras, 2015). A 50% reduction in forest cover in the CMIP6 models causes a  $-11\%$  to  $+2\%$  change in precipitation in the Amazon, with large uncertainty in the response of regional moisture convergence to land cover change (Luo et al., 2022).

Most previous studies have assessed hypothetical and extreme land cover changes, such as complete Amazon deforestation (Luo et al., 2022; Spracklen & Garcia-Carreras, 2015), and much less is known about the impacts of realistic land cover changes. Studies of more realistic deforestation patterns suggest complex and substantial impacts on precipitation (Alves et al., 2017; Commar et al., 2023; de Sales et al., 2020; Khanna et al., 2017; Lima et al., 2023; Sierra et al., 2023; Spera et al., 2020) that are not fully understood. Additional studies of the impacts of recent land cover change in the Amazon are urgently needed.

Forest cover change in the Amazon can also influence the hydrological regime in downwind regions through large-scale atmospheric circulations. The Amazon serves as the moisture source for southeastern South America (Drumond et al., 2014). Results from offline tracer models have demonstrated the importance of the Amazon as a moisture source for downwind forests (Staal et al., 2018) and parts of southeastern South America (Ruiz-Vásquez et al., 2020; Spracklen et al., 2018; van der Ent et al., 2010; Zemp et al., 2014). However, these offline studies neglect the atmospheric response to land cover change, which could amplify or suppress the precipitation responses (Baudena et al., 2021). Climate models include atmospheric responses to land-use change but with large intermodel variability (Luo et al., 2022). New developments in atmospheric moisture tracking within climate models provide an unprecedented opportunity to disentangle precipitation responses to land cover changes (Baudena et al., 2021; Dominguez et al., 2022).

To increase our knowledge of the biophysical effects of deforestation on precipitation and the moisture cycle in the Brazilian Amazon, we carried out simulations using the state-of-the-art water vapor tracer (WVT) embedded in the regional coupled Weather Research and Forecasting (WRF) model. This online model simulates the changes in large-scale atmospheric circulations due to forest cover change, overcoming the limitation caused by offline models. We used embedded water tracers to track sources of moisture and allocate changes in precipitation to local and non-local sources. To ensure that we simulated realistic changes in forest cover, that included deforestation, forest regrowth and greening trends, we used multiple satellite data sets to describe the forest cover change. We focused our study on Mato Grosso and Rondônia in southern Brazil for the period 2001 to 2015. We selected these states because they together account for 30% of Brazilian Amazon deforestation in recent decades

(PRODES; Almeida et al., 2022). We designed factorial experiments, with one undergoing forest cover change but the other not, allowing us to separate the effects of forest cover change on climate. Our aim is to deepen our understanding of the local and non-local effects of recent forest cover change on the terrestrial water balance in the Brazilian Amazon and to provide information at a scale that can inform state-to-national-level forest and climate policy.

## 2. Materials and Methods

### 2.1. WRF-WVT Model

The WVT (Insua-Costa & Miguez-Macho, 2018) embedded within the WRF model (version 4.3.3) is used in this study. The simulation domain is centered at 50°W, 15°S, covering the Brazilian Amazon and neighboring regions (Figure 1a). Rondônia and Mato Grosso are chosen as the moisture-tagged area, because they have some of the largest recent deforestation areas in the Brazilian Amazon (Leite-Filho et al., 2021). The evapotranspiration within the tagged area is tagged and tracked by the WVT, and then the WRF-WVT allows us to track water vapor which is evapotranspired from the tagged region until it falls as precipitation.

Our model setup includes 350 grids in the west–east direction and 250 grids in the south–north direction, with a grid space of 25 km. There are 40 vertical levels, with the bottom level following the terrain and the top level fixed at 50 hPa. The boundary and initial conditions of the simulation are derived from the Final Operational Model Global Tropospheric Analyses data at a horizontal resolution of 1° × 1° and 6-hr intervals (National Centers for Environmental Prediction/National Weather Service/NOAA/U.S. Department of Commerce, 2000). WRF-WVT requires the Yonsei University scheme (Hong et al., 2006) for the planetary boundary layer, the Single-Moment 6-class scheme (Hong & Lim, 2006) for microphysics, and the Kain–Fritsch scheme (Kain, 2004) for convection. For the land component, the Noah-MP scheme (Niu et al., 2011) is used. Noah-MP calculates evapotranspiration by explicitly representing three key processes: soil surface evaporation, canopy interception loss, and plant transpiration. These processes are modeled using an analogy to Ohm's law, incorporating aerodynamic and stomatal resistances to water vapor and carbon fluxes within and above plant canopies. Transpiration is regulated by stomatal resistance, which is connected to photosynthesis, itself influenced by the root zone soil moisture. Noah-MP assumes roots are uniformly distributed vertically, with root depth varying based on vegetation type (Ma et al., 2017). The Rapid Radiative Transfer Model scheme (Iacono et al., 2008) is used for shortwave and longwave radiation.

### 2.2. Experimental Design

To isolate the biophysical effects of forest cover change in Mato Grosso and Rondônia, we conducted three 15-year simulations: a control simulation (CTL), and two deforestation simulations (DEF and DEF\_al). All simulations were run continuously from 1 January 2001 to 31 December 2015, with identical model configurations except for differences in land cover and surface biophysical properties within Mato Grosso and Rondônia. Land cover and surface properties were prescribed from satellite data (Section 2.2) and include snow-free albedo, green vegetation fraction, leaf area index (LAI), and aerodynamic roughness length. In the CTL simulation, land cover and surface properties within Mato Grosso and Rondônia were fixed at 2001 values. In the DEF simulation, land cover and surface properties were allowed to vary annually or monthly within the simulation domain. To better attribute changes in land surface properties to specific biophysical processes, we conducted a sensitivity simulation (DEF\_al) to assess the relative contributions of ET and albedo changes. The DEF\_al simulation is identical to DEF, except albedo values within Mato Grosso and Rondônia are fixed at 2001 values.

The first year of each simulation was used as a spin-up period to allow the model to reach equilibrium, and was therefore excluded from the analysis. We quantified the biophysical effects of forest cover change by calculating the 14-year (2002–2015) mean differences between simulations. We calculated 95% confidence intervals based on 1,000 bootstrapped resamples. The impact of forest cover change was calculated as the difference between CTL and DEF (DEF minus CTL) simulations. The DEF\_al simulation further allows us to isolate the role of albedo changes, disentangling the different ways that deforestation alters land surface properties. We focus our analysis on the dry season when reductions in rainfall have the biggest impact. We define the dry season as May to October, which are the six driest months. Previous studies have used similar definitions of the dry season; Bagley et al. (2014) defined the dry season as May to September. Defining the dry season as the driest 3 months (August to October) leads to similar results and does not change our conclusions.

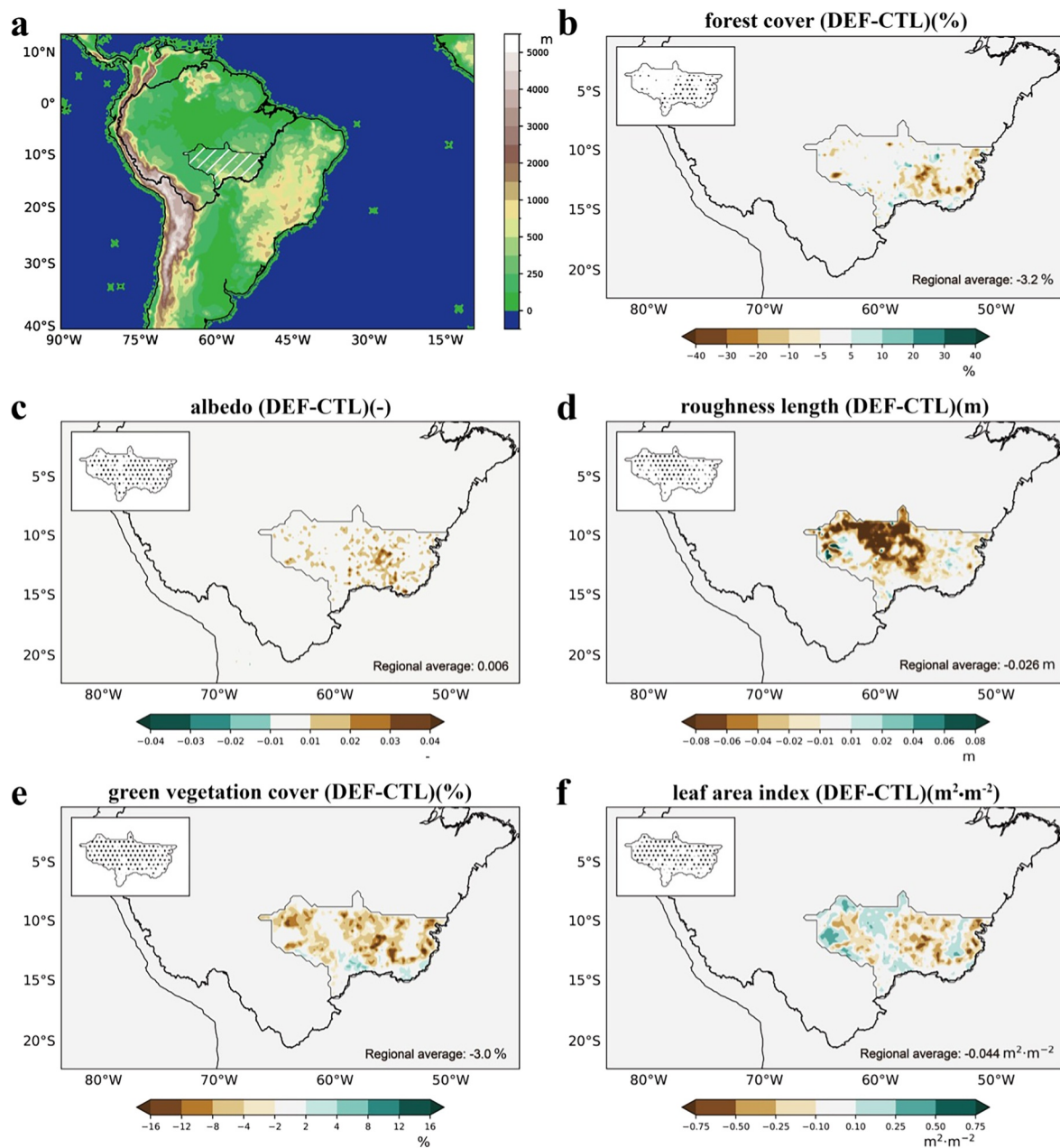


**Figure 1.** Land surface properties. (a) The simulation domain. The color shading denotes the altitude (unit: m). The hatching denotes Mato Grosso and Rondônia where the evapotranspiration is tagged and land surface properties differ between the two simulations. 14-year (2002–2015) mean differences in the dry season mean: (b) forest cover (unit: %); (c) albedo; (d) roughness length (unit: m); (e) green vegetation cover (unit: %); and (f) leaf area index (unit:  $\text{m}^2\cdot\text{m}^{-2}$ ) between the DEF and CTL simulations (DEF minus CTL). In panels (b–f), the map of the statistical significance test is shown in the upper-left corner of each panel. The stippling denotes that the local change is statistically significant at the 95% confidence level using the two-tailed Student's *t*-test. The 14-year mean value averaged over the tagged region is shown in the lower-right corner of each panel.

Figure 1 shows the satellite-observed changes in the dry season (May to October) mean land surface properties from 2002 to 2015. The dry season mean forest cover (FC), green vegetation fraction (GREENFRAC) and leaf area index (LAI) are significantly ( $p < 0.01$ ) lower in DEF than in CTL, with a larger reduction in the southeastern region. Regional average forest cover decreases by an average of 3.2% over this period, closely matching the deforestation rate reported by the PRODES (Figure S2 in Supporting Information S1). All the surface properties change significantly in the dry season ( $p < 0.01$ ). Regional average albedo increases by 0.006 with the largest increase in the southeast. Regional average roughness length (*Z*0) decreases by 0.026 m. Regional average LAI is

reduced by  $0.04 \text{ m}^2\text{-m}^{-2}$  but increases in regions with no forest cover loss. Annual mean and wet season changes in surface properties (Figure S3 in Supporting Information S1) show similar patterns but with stronger increases in LAI.

### 2.3. Attribution of the Precipitation Changes Caused by Forest Cover Change

To reveal the mechanisms for precipitation responses to forest cover change, an attribution method based on the moisture budget equation (Seager et al., 2007) is used.

At monthly scales, the precipitation response to forest cover change can be expressed as:

$$\delta\text{Pr} = \delta\text{ET} + \delta\text{MFC} + \delta\text{TEC} \quad (1)$$

where  $\delta$  indicates the difference between the CTL and DEF simulations (DEF minus CTL), Pr is the monthly mean precipitation (mm), ET is the monthly mean evapotranspiration (mm), MFC is the monthly mean moisture flow convergence (mm) and TEC is the transient eddy convergence (mm). The MFC is determined by monthly mean wind and moisture fields, while the TEC is determined by high-frequency (e.g., hourly and daily) wind and moisture fields. Since  $\delta\text{ET}$  and  $\delta\text{MFC}$  can mostly explain  $\delta\text{Pr}$  (Y. Liu et al., 2023),  $\delta\text{TEC}$  is omitted and is not further analyzed.

$\delta\text{MFC}$  can be further decomposed into the dynamic component ( $\delta\text{MCD}$ ), the thermodynamic component ( $\delta\text{TH}$ ), and the covariant component ( $\delta\text{COV}$ ), expressed as:

$$\delta\text{MFC} = \delta\text{TH} + \delta\text{MCD} + \delta\text{COV} \quad (2)$$

$$\delta\text{MCD} = -\frac{1}{\rho_w g} \int_0^{\text{ps}} \nabla \cdot (\bar{q}\delta\bar{u}) \text{d}p \quad (3)$$

$$\delta\text{TH} = -\frac{1}{\rho_w g} \int_0^{\text{ps}} \nabla \cdot (\bar{u}\delta\bar{q}) \text{d}p \quad (4)$$

$$\delta\text{COV} = -\frac{1}{\rho_w g} \int_0^{\text{ps}} \nabla \cdot (\delta\bar{q}\delta\bar{u}) \text{d}p \quad (5)$$

where  $\rho_w$  is the density of water ( $\text{kg}\cdot\text{m}^{-3}$ ),  $g$  is the acceleration due to gravity ( $9.80 \text{ m}\cdot\text{s}^{-2}$ ),  $\nabla$  is the horizontal divergence operator,  $u$  is horizontal vector wind ( $\text{m}\cdot\text{s}^{-1}$ ),  $q$  is atmospheric specific humidity, and the overbar denotes the monthly mean value. The moisture convergence is integrated over pressure ( $p$ ) from the top of the atmosphere ( $p = 50 \text{ hpa}$ ) to the surface (ps). The terms  $\delta\text{MCD}$ ,  $\delta\text{TH}$ , and  $\delta\text{COV}$  can be interpreted as  $\delta\text{MFC}$  caused by horizontal wind anomalies, specific humidity anomalies and the product of specific humidity and horizontal wind anomalies, respectively. Based on these equations, we can determine the impacts of forest cover change on the components of the water budget.

We calculate precipitation efficiency (PE), defined as precipitation divided by atmospheric precipitable water (PW):

$$\text{PE} = \frac{\text{Pr}}{\text{PW}} \quad (6)$$

Using WVT, total precipitation can be separated into precipitation originating from evapotranspiration within the tagged region (tagged precipitation) and precipitation sourced from moisture inflow transported by atmospheric circulation (untagged precipitation). For tagged and untagged precipitation, PW is calculated as the corresponding precipitable water:

$$\text{PE}_{\text{tagged}} = \frac{\text{Pr}_{\text{tagged}}}{\text{PW}_{\text{tagged}}} \quad (7)$$

$$PE_{\text{untagged}} = \frac{Pr_{\text{untagged}}}{PW_{\text{untagged}}} \quad (8)$$

Since PW is relatively stable while precipitation is variable over smaller space and time scales, higher PE indicates an effective local dynamic mechanism that facilitates the condensation process leading to precipitation.

Based on Equation 6, the changes in precipitation can be attributed to changes in PE and changes in PW, and the contribution can be calculated as:

$$\rho_{PE} = \frac{\delta PE * PW_{CTL}}{\delta Pr} \quad (9)$$

$$\rho_{PW} = \frac{\delta PW * PE_{CTL}}{\delta Pr} \quad (10)$$

Similarly,  $\rho_{PE}$  and  $\rho_{PW}$  can also be applied to tagged and untagged precipitation as:

$$\rho_{PE}^{\text{tagged}} = \frac{\delta PE_{\text{tagged}} * PW_{CTL}^{\text{tagged}}}{\delta Pr} \quad (11)$$

$$\rho_{PW}^{\text{tagged}} = \frac{\delta PW_{\text{tagged}} * PE_{CTL}^{\text{tagged}}}{\delta Pr} \quad (12)$$

$$\rho_{PE}^{\text{untagged}} = \frac{\delta PE_{\text{untagged}} * PW_{CTL}^{\text{untagged}}}{\delta Pr} \quad (13)$$

$$\rho_{PW}^{\text{untagged}} = \frac{\delta PW_{\text{untagged}} * PE_{CTL}^{\text{untagged}}}{\delta Pr} \quad (14)$$

#### 2.4. Satellite Data

Land cover and surface properties were prescribed from satellite observations. Specifically, land cover data were obtained from the MODIS land cover type product (MCD12C1, version 6; Friedl & Sulla-Menashe, 2015), which classifies land into 17 categories based on the International Geosphere-Biosphere Program scheme, provided at a 0.05° spatial resolution and updated annually in the DEF simulation from 2001 to 2015. These 17 categories are further classified into forest categories (e.g., evergreen needleleaf forest, evergreen broadleaf forest etc.) and non-forest categories (e.g., grassland, croplands, barren etc.), and they proportionally cover each grid cell. Forest cover is calculated as the sum of the forest categories. The change in forest cover is used to compare against reported deforestation rates. Surface properties (such as LAI, ET etc) are prescribed from other satellite data or calculated separately. The LAI data were sourced from the reprocessed MODIS version 6 LAI data sets, known for their superior spatial and temporal continuity (Yuan et al., 2011, 2020), and were provided at a 0.05° spatial resolution with monthly updates. The fraction of absorbed photosynthetically active radiation, used as a proxy for the green vegetation fraction, was derived from the Global Land Surface Satellite product (Ge et al., 2020; Kumar et al., 2014; Z. Y. Liu et al., 2006; Xiao et al., 2015, 2018) provided at a 0.05° spatial resolution and monthly intervals. Snow-free albedo data were taken from the gap-filled, snow-free MODIS Bidirectional Reflectance Distribution Function and Albedo product (MCD43GF version 6; Schaaf, 2019), provided at a 500 m spatial resolution and 8-day intervals, which were aggregated into monthly values for consistency. Finally, roughness length was estimated using remote-sensed LAI, canopy height, and plant functional type-dependent canopy morphological characteristics (Y. Liu et al., 2021) and provided at a 0.05° spatial resolution with monthly updates.

Non-forest vegetation, such as grasslands and croplands typically have lower dry season ET, green vegetation fraction, LAI and roughness, but higher albedo compared to tree-dominated areas. Trees have deep roots allowing them to maintain green leaves and higher rates of ET throughout the dry season.

We evaluate the WRF-WVT for precipitation and evapotranspiration in the tagged area using gridded precipitation data from the Tropical Rainfall Measuring Mission (TRMM; Huffman et al., 2016) data set and

evapotranspiration data from the Moderate Resolution Imaging Spectroradiometer (MODIS) product (MOD16A2; Running et al., 2021) (Figure S1 in Supporting Information S1). The WRF simulated annual cycles of precipitation coincide well with the TRMM data, and the magnitudes of model biases are comparable to those produced by the well-tuned WRF model in prior studies (Chug et al., 2022; Dominguez et al., 2022).

WRF simulations capture the seasonal cycle of precipitation in the southern Amazon (Figure S1 in Supporting Information S1). WRF overestimates precipitation during the wetter months (November to April) as commonly observed in studies of the Amazon using the WRF model (Dominguez et al., 2022; Gomes et al., 2022; Tai et al., 2024). This bias may stem from the convective parameterization scheme (Kain–Fritsch scheme) generating errors when handling convective-scale precipitation at the model's spatial resolution. WRF better simulates precipitation during the drier months (May to October), and the bias between WRF and TRMM is not significant ( $p > 0.2$ ). WRF also captures spatial patterns of dry season evapotranspiration and precipitation, with greater evapotranspiration and precipitation over regions of forest cover over the study region (Figures S1c and S1d in Supporting Information S1). So, in this study, we focus on the driest 6 months (May to October) which we define as the dry season. We also report results for the driest 3 months (June to August).

### 3. Results and Discussion

#### 3.1. Biophysical Impacts of Forest Loss on the Terrestrial Water Balance

Figure 2 shows the dry season mean evapotranspiration (ET) and precipitation (Pr) response to forest loss. The spatial distributions of changes in ET and Pr (Figures 2a–2d) are consistent with changes in surface properties (Figure 1). In areas with greater forest loss, changes in ET are significant ( $p < 0.05$ ) and more pronounced (Figure 2b). At a regional scale across Mato Grosso and Rondônia, forest loss caused a significant reduction in regionally averaged dry season ET of  $-4.2 \pm 0.9$  mm-month<sup>-1</sup> ( $\pm 95\%$  CI) (Figure 2e; Figure S4a in Supporting Information S1). Forest loss has also caused a significant reduction in regional dry season precipitation of  $-5.2 \pm 4.2$  mm-month<sup>-1</sup> (95% CI) (Figure S4b in Supporting Information S1). Unlike ET, the spatial patterns of Pr changes are not significant ( $p > 0.05$ ) likely due to the limited forest loss (3.20%, Figure 1b) and the large interannual variability in rainfall over the region (Figure S1 in Supporting Information S1).

Forest loss of 3.2% causes a simulated relative change in dry season regional ET of  $-3.5 \pm 0.8\%$  and precipitation of  $-5.4 \pm 4.4\%$  (Figure 2e). The reduction in precipitation during the driest 3 months (June to August) is similar at  $-4.6\%$ . Our results suggest that deforestation reduces precipitation in the southern Amazon, in-line with previous regional modeling studies (e.g., Bagley et al., 2014). We simulated the impacts of recent forest loss and show that this has likely led to a significant reduction in regional precipitation. We estimate a  $-1.69\%$  change in dry season precipitation per percentage point of forest loss, with lower sensitivity in the wet season ( $-0.41\%$ ) and the annual mean ( $-0.68\%$ ) (Figure S5 in Supporting Information S1). Previous studies have reported a wide range of sensitivities of precipitation to forest cover loss in the Amazon. Baudena et al. (2021) analyzed back trajectories and reanalysis meteorological data and estimated a  $-0.55\%$  to  $-0.7\%$  change in annual mean precipitation per percentage point of forest loss, with no strong seasonal pattern. Duku and Hein (2023) analyzed reanalysis data over the Amazon and estimated a  $-0.68\%$  change in precipitation per percentage point of forest loss. Smith, Baker, and Spracklen et al. (2023) and Smith, Robertson, et al. (2023) analyzed satellite data across regions of tropical forest loss and reported a  $-0.2\%$  change in precipitation per percentage point of forest loss. Spracklen and Garcia-Carreras (2015) reported a multi-model annual mean change of  $-0.16\%$  per percentage point of forest loss for simulations of complete Amazon deforestation. Luo et al. (2022) analyzed deforestation simulations for the Amazon in the CMIP6 models of and reported a  $-0.09\%$  change in precipitation per percentage point of forest loss. Constraining the sensitivity of precipitation to forest loss is crucial for improving regional climate projections and informing sustainable forest management.

In our simulations, forest loss caused larger absolute ( $-5.2$  mm-month<sup>-1</sup>) and relative ( $-5.4\%$ ) reductions in precipitation compared to ET ( $-4.2$  mm-month<sup>-1</sup>,  $-3.5\%$ ) (Figure 2e). This suggests that assuming precipitation decreases proportionally to the transpired portion of atmospheric moisture is likely to underestimate the effects of deforestation on precipitation (Baudena et al., 2021; Makarieva et al., 2023). The greater reduction in precipitation compared to the local reduction in ET is due to atmospheric responses to forest cover change, which we explore in the following sections.

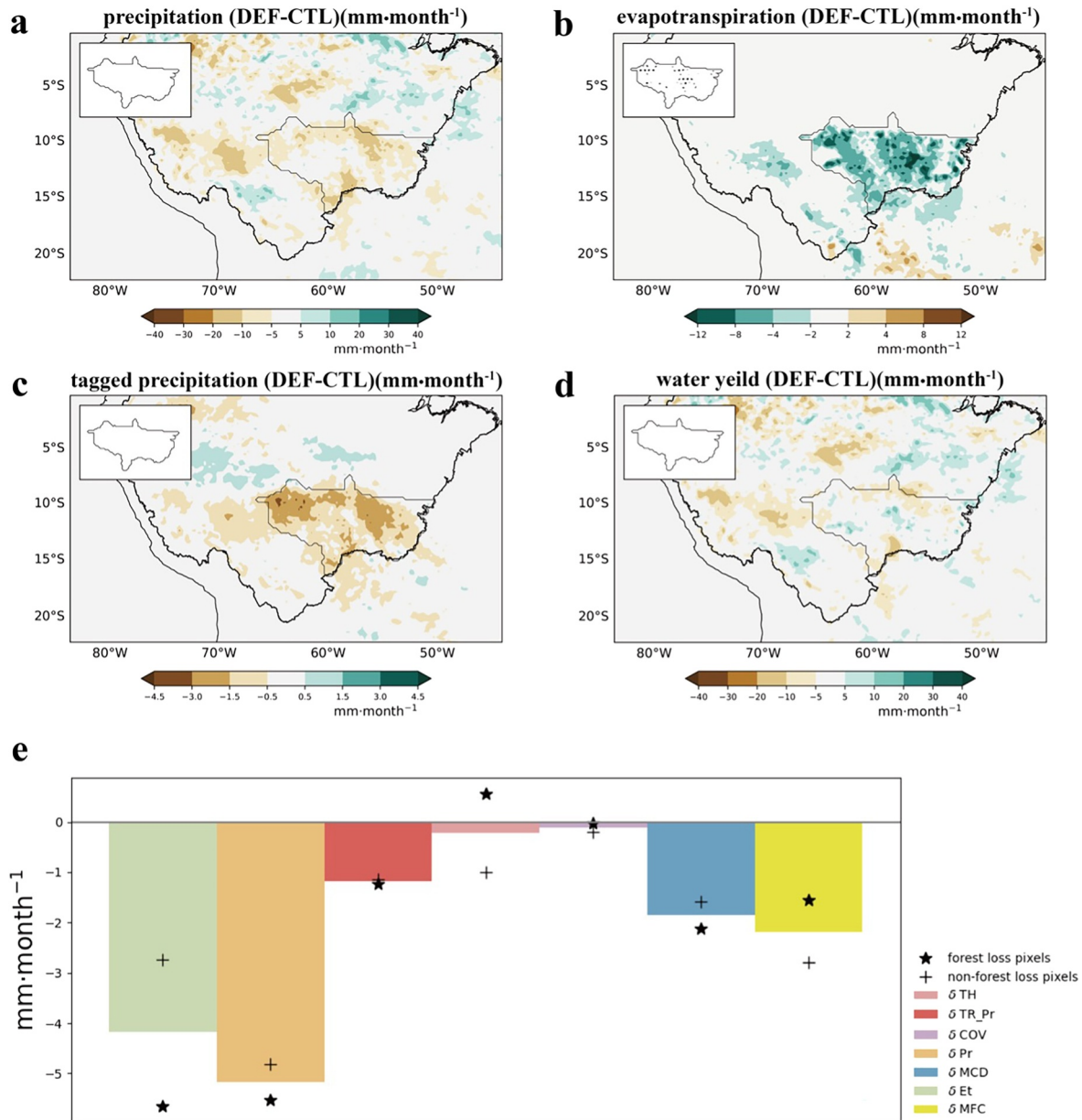


**Figure 2.** Impacts of forest loss on the dry season regional water cycle. All values are calculated from the difference between the DEF and CTL simulations (DEF minus CTL) over the 14-year period (2002–2015). (a) Precipitation (unit: mm-month<sup>-1</sup>), (b) evapotranspiration (unit: mm-month<sup>-1</sup>), (c) tagged precipitation (unit: mm-month<sup>-1</sup>), and (d) water yield (unit: mm-month<sup>-1</sup>). The map of the statistical significance test is shown in the upper-left corner of each panel. The stippling denotes that the local change is statistically significant at the 95% confidence level using the two-tailed Student's *t*-test. (e) The changes in 14-year (2002–2015) mean dry season precipitation ( $\delta Pr$ ; orange bar), evapotranspiration ( $\delta Et$ ; green bar), recycling precipitation ( $\delta TR_{Pr}$ ; red bar), mean flow convergence ( $\delta MFC$ ; yellow bar), the dynamic component of  $\delta MFC$  ( $\delta MCD$ ; blue bar), the thermodynamic component of  $\delta MFC$  ( $\delta TH$ ; pink bar), and the covariant component of  $\delta MFC$  ( $\delta COV$ ; purple bar) due to land cover changes (DEF minus CTL) averaged over Mato Grosso and Rondônia. The regional average results are shown in bars, and changes over pixels with and without forest loss are shown in black star and black cross respectively. All variables are shown with units of mm-month<sup>-1</sup>.

Reductions in both ET and Pr are greater over pixels with forest loss (Figure 2e) compared to pixels without loss. Pixels without forest loss also experience a reduction in ET due to neighboring forest loss, driven by reductions in regional precipitation. This further suggests an important impact of atmospheric responses to forest loss.

Figure 3 shows a schematic of the dry season water vapor cycle in the DEF and CTL simulations. Forest loss (DEF-CTL) causes a reduction in all components of the water vapor cycle. Forest loss causes a reduction in both incoming (−9.7 mm-month<sup>-1</sup>) and outgoing (−8.3 mm-month<sup>-1</sup>) atmospheric moisture resulting in a net

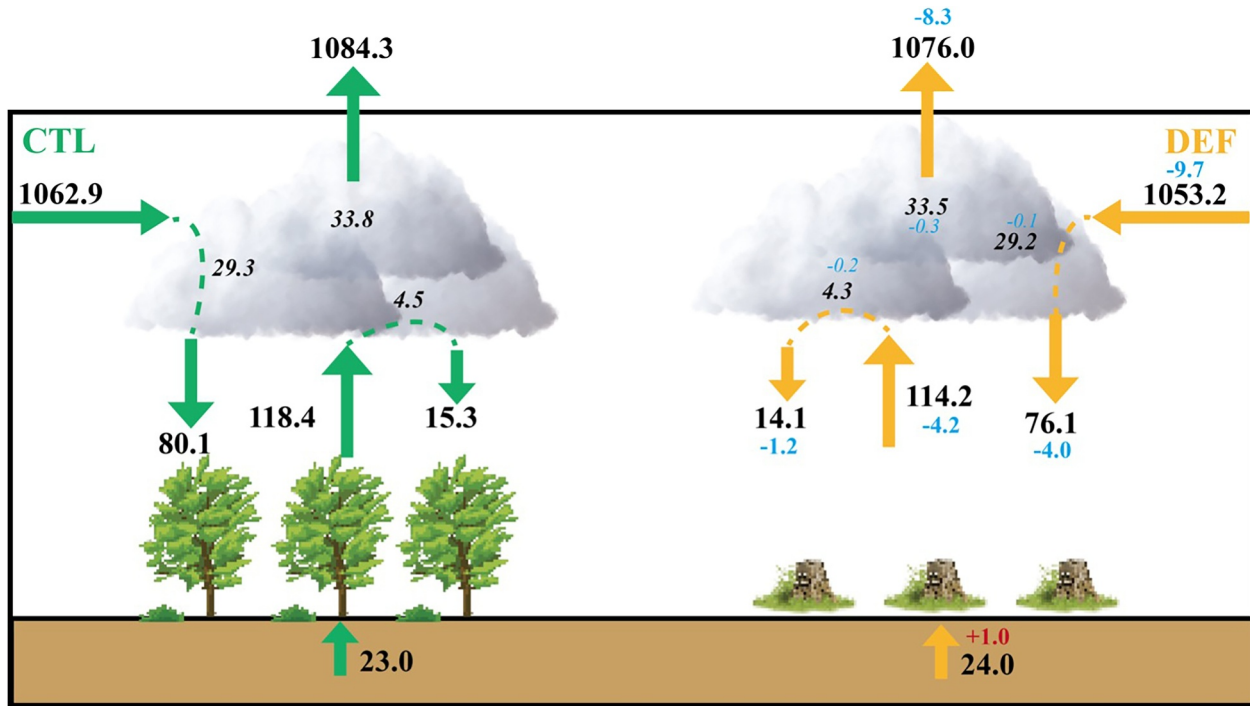


**Figure 3.** Schematic diagram of the impacts of forest loss on the atmospheric water cycle over Mato Grosso and Rondônia during the dry season. Arrows denote components of the atmospheric water vapor cycle in CTL (green, unit:  $\text{mm}\cdot\text{month}^{-1}$ ) and DEF (orange, unit:  $\text{mm}\cdot\text{month}^{-1}$ ) simulations. The components are land storage (soil or groundwater store) plus runoff (water yield; precipitation minus evapotranspiration); ET; water vapor inflow and outflow; tagged precipitation and nonlocal precipitation (precipitation originating from water vapor inflow, indicated by dashed line linking water inflow). The numbers in black indicate the amount of the water cycle components. The numbers in blue (red) indicate the decrease (increase) in the water cycle components due to forest cover changes (DEF minus CTL). The italic numbers denote precipitable water and its tagged and untagged parts (unit: mm).

reduction in moisture inflow ( $-1.4 \text{ mm}\cdot\text{month}^{-1}$ ). This net reduction in moisture inflow amplifies the reduction in atmospheric moisture due to reduced ET and accounts for 25% of the total reduction in moisture due to both reduced ET and reduced moisture inflow ( $-5.6 \text{ mm}\cdot\text{month}^{-1}$ ). The reduction in Pr ( $-5.2 \text{ mm}\cdot\text{month}^{-1}$ ) accounts for 93% of the total reduction in moisture.

Moisture fluxes into the region can be further diagnosed as changes in MFC (Equation 1) which can be decomposed as changes in MCD, COV and TH. Forest loss reduces MFC ( $-2.2 \text{ mm}\cdot\text{month}^{-1}$ ; Figure 2e), larger than the net change in moisture inflow ( $-1.4 \text{ mm}\cdot\text{month}^{-1}$ ; Figure 3). The change in MFC is dominated by a reduction in the horizontal wind anomalies ( $\delta\text{MCD}$ ,  $-1.8 \text{ mm}\cdot\text{month}^{-1}$ , 81.8%) with smaller contributions from the covariant component ( $\delta\text{COV}$ ,  $-0.1 \text{ mm}\cdot\text{month}^{-1}$ , 4.5%) and thermodynamic component ( $\delta\text{TH}$ ,  $-0.2 \text{ mm}\cdot\text{month}^{-1}$ , 9.1%). This shows that the main cause for reduced moisture inputs is due to changing atmospheric circulation.

Using WVT, we attributed the changes in precipitation to changes in local moisture (changes in Pr sourced from changes in ET from the tagged region) and nonlocal moisture (changes in Pr sourced from changes in non-local moisture from outside the tagged region). The  $4.0 \text{ mm}\cdot\text{month}^{-1}$  reduction in untagged precipitation accounts for 76.9% ( $4.0 \text{ mm}\cdot\text{month}^{-1}/5.2 \text{ mm}\cdot\text{month}^{-1}$ ) of changes in total precipitation. The reduction in tagged precipitation accounts for the remaining 23.1% ( $1.2 \text{ mm}\cdot\text{month}^{-1}/5.2 \text{ mm}\cdot\text{month}^{-1}$ ). Therefore, a reduction in precipitation sourced from non-local moisture is the main cause of the precipitation reduction due to forest loss in Mato Grosso and Rondônia during the dry season. So, although the reduction in non-local moisture only accounts for 25% of the net reduction in atmospheric moisture, 77% of the reduction in precipitation is from moisture outside the tagged region.

To explore changes in precipitation further, we calculated changes in precipitation efficiency (PE) and precipitable water (PW) (Table 1). Forest loss reduces PE by 4.6% and PW by 0.9%. The contribution of PE reduction to

**Table 1**  
14-Year (2002–2015) Mean Changes in Dry Season Precipitation ( $Pr$ , Unit:  $\text{mm}\cdot\text{month}^{-1}$ ), Precipitable Water ( $PW$ , Unit:  $\text{mm}$ ), and Precipitation Efficiency ( $PE$ , Unit:  $\text{month}^{-1}$ ) Due To Forest Loss

	CTL	DEF	DEF-CTL	$\rho$ (%)
$Pr_{\text{total}}$	95.4	90.2	-5.2 (-5.5%)	
$Pr_{\text{untagged}}$	80.1	76.1	-4.0 (-5.0%)	76.9%
$Pr_{\text{tagged}}$	15.3	14.1	-1.2 (-7.8%)	23.1%
$PW_{\text{total}}$	33.8	33.5	-0.3 (-0.9%)	16.3%
$PW_{\text{untagged}}$	29.3	29.2	-0.1 (-0.3%)	5.3%
$PW_{\text{tagged}}$	4.5	4.3	-0.2 (-4.4%)	13.1%
$PE_{\text{total}}$	2.82	2.69	-0.13 (-4.6%)	84.5%
$PE_{\text{untagged}}$	2.73	2.61	-0.12 (-4.4%)	67.6%
$PE_{\text{tagged}}$	3.40	3.28	-0.12 (-3.5%)	10.4%

Note. Calculated as the DEF simulation minus the CTL simulation. The numbers in parentheses represent relative changes. The contribution shows the proportion ( $\rho$ ) of the total precipitation change caused by this factor.

total precipitation change ( $\rho_{PE}$ ) is 84.5% and the contribution of precipitable water reduction ( $\rho_{PW}$ ) is 16.3%. Thus, the main reason for reduced precipitation is due to a reduction in precipitation efficiency.

We also calculated PE separately for tagged and untagged water vapor. Reduction in tagged precipitable water ( $\rho_{PW}^{\text{tagged}}$ ) contributes 13.1% of the reduction in total precipitation and the decrease in PE of tagged moisture ( $\rho_{PE}^{\text{tagged}}$ ) contributes 10.4% of the reduction in total precipitation. Reduction in untagged PW ( $\rho_{PW}^{\text{untagged}}$ ) contributes 5.3% of the reduction in total precipitation, while a decrease in PE of untagged moisture ( $\rho_{PE}^{\text{untagged}}$ ) contributes 67.6% of the reduction in precipitation. Therefore, the reduction in PE of untagged precipitation predominantly drives the total precipitation decrease in the dry season.

To better understand the response of PE to changes in surface parameters, we classify the daily precipitation from the 14-year DEF and CTL simulations according to their precipitable water content and compare differences in the mean precipitation rate, total cumulative precipitation, and precipitation frequency under the same precipitable water content (Figure 4). Reductions in total cumulative precipitation are greatest for higher PW. Under high PW, forest loss reduced total cumulative precipitation but increased the mean daily

precipitation rate. This means that despite mean reduction in PE the daily PE in the DEF simulation can exceed that in the CTL simulation for high PW. Deforestation-induced intensification of storms has also been proposed in West Africa (Taylor et al., 2022). However, due to the drier atmosphere in the DEF simulation, the frequency of high PW decreases. Consequently, seasonal cumulative precipitation is reduced, which, on a seasonal scale, manifests as a decrease in PE.

### 3.2. Mechanism for the Water Vapor Cycle Response to Forest Loss

To examine the potential mechanisms of precipitation change, we examined the diurnal cycle of changes in surface turbulent and net downward surface radiative fluxes over Mato Grosso and Rondônia (Figure 5d). Forest loss leads to reduced shortwave radiation (due to increased albedo) and reduced latent heat and increased sensible heat (due to reduced ET), with changes in all fluxes peaking at noon (Figure 5d). These changes lead to increased regional average dry season surface air temperature by  $0.12^\circ\text{C}$  with warming simulated throughout the day

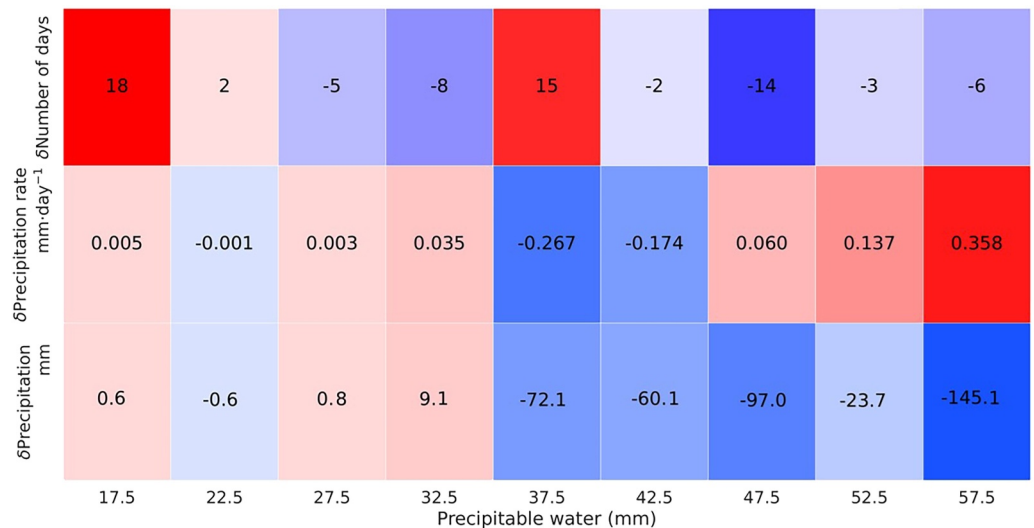


**Figure 4.** Impacts of forest cover change (DEF minus CTL) on number of precipitation days, mean precipitation rate (unit:  $\text{mm}\cdot\text{day}^{-1}$ ), and cumulative precipitation (mm) under different precipitable water contents in the dry season.

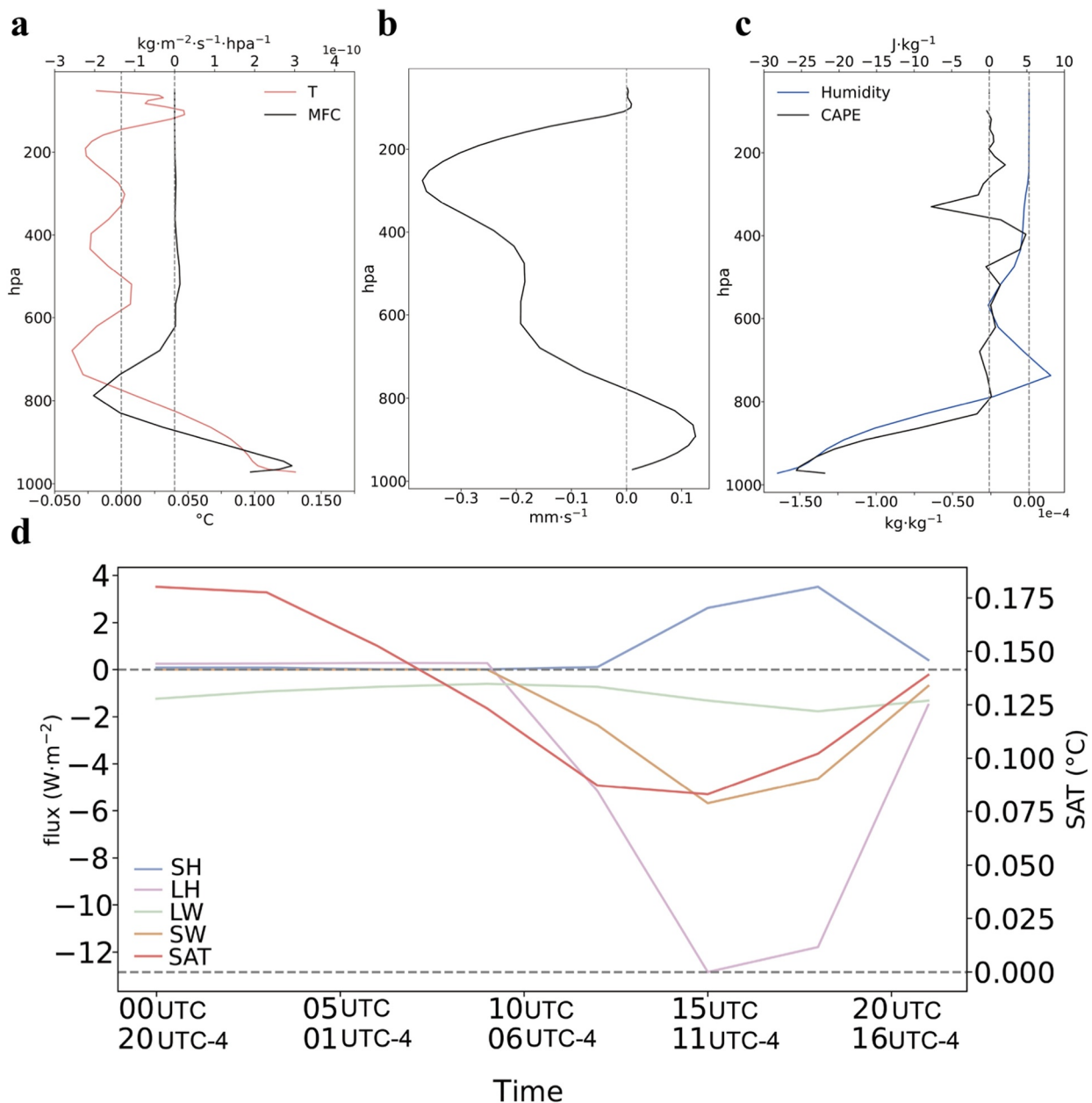


**Figure 5.** (a–c) The vertical structure of atmospheric responses to forest cover change in the dry season (a) mean flow convergence (black; unit:  $kg \cdot m^{-2} \cdot s^{-1} \cdot hPa^{-1}$ ) and air temperature (red; unit:  $^{\circ}C$ ), (b) vertical velocity (unit:  $mm \cdot s^{-1}$ ), and (c) convective available potential energy (black; unit:  $J \cdot kg^{-1}$ ) and specific humidity (blue; unit:  $kg \cdot kg^{-1}$ ). All the results are shown for forest loss (DEF minus CTL) calculated as the average of 14-year (2002–2015) simulations. (d) 14-year (2002–2015) mean diurnal cycle of changes (DEF minus CTL) in turbulent and radiative heat fluxes (unit:  $W \cdot m^{-2}$ ) including sensible heat (SH), latent heat (LH), longwave (LW) and shortwave (SW) radiation and surface air temperature (SAT, unit:  $^{\circ}C$ ) averaged over Mato Grosso and Rondônia in the dry season. UTC-4 is local time.

(Figure 5a). This is equivalent to  $0.04^{\circ}C$  warming per percentage point of forest cover loss, within the range of warming ( $0.01$ – $0.07^{\circ}C$  per percentage point of forest loss) reported from satellite studies of tropical forest loss (Alkama & Cescatti, 2016; Baker & Spracklen, 2019; Butt et al., 2023; Duveiller et al., 2020; Smith, Robertson, et al., 2023).

We also examined the vertical structure of temperature, humidity, vertical motion and convective available potential energy (CAPE) above Mato Grosso and Rondônia (Figures 5a–5c). Surface warming (Figure 5a) enhances vertical motion in the lower troposphere (1,000–900 hPa) (Figure 5b). Rising surface air combined with lower surface roughness results in increased low-level moisture flux convergence (Figure 5a). However, this

moisture convergence does not compensate for the reduction in moisture due to reduced ET resulting in a reduction in lower troposphere specific humidity (Figure 5c). The reduction in humidity dominates over surface warming and CAPE is reduced (Figure 5c), suppressing convection, as indicated by reduced vertical motion above 800 hPa (Figure 5b). The net moisture flux is dominated by reduced moisture inflow in the mid-troposphere (Figure 5a), resulting in a reduction in column integrated MFC (Figure 2). Weaker convection tends to reduce precipitation, resulting in cooling above 800 hPa due to the reduced latent heat energy released from water vapor condensation (Figure 5a). This causes mid-tropospheric subsidence (Figure 5b) leading to reduced moisture flux convergence around 800 hPa (Figure 5a). This alteration in the dry season water vapor circulation structure due to forest loss is consistent with the findings based on satellite data and reanalysis data (Xu et al., 2022).

This key role of ET in driving precipitation changes is confirmed by an additional deforestation simulation where albedo was fixed at the 2001 values (DEF\_al; Figure S6 in Supporting Information S1). Under this simulation, forest loss results in smaller reductions in both ET (−1.4%) and precipitation (−4.0%) compared to DEF case. The smaller reduction in ET causes smaller reductions in LH (−5 W·m<sup>−2</sup>) and less surface warming (0.02°C). Overall, the consistent reduction in precipitation, even when albedo remains fixed, indicates that changes to the moisture budget—rather than albedo effects—are the dominant drivers of reduced precipitation.

In our study reductions in PE, driven by reductions in ET drying the lower atmosphere and reducing convection, dominate deforestation-induced reductions in dry season precipitation in the southern Amazon. Langenbrunner et al. (2019) also found that reductions in ET (driven by the physiological response of the Amazon forest to elevated CO<sub>2</sub>) resulted in reduced convection and precipitation. Wright et al. (2017) reported observational evidence that forest transpiration helped initiate convection, particularly during the dry-to-wet season transition. Deforestation causes warming (which acts to increase CAPE) and drying (which acts to reduce CAPE) of the lower atmosphere. Whether these changes lead to increased or reduced CAPE may depend on the magnitude of the warming and drying caused by forest loss. Other modeling studies have found that reductions in CAPE cause small changes in precipitation in the Amazon because the simulated atmosphere was highly unstable and prone to convection (Swann et al., 2015). This suggests that the modeled response is likely to be sensitive to the background climate in the model as well as the convection scheme. A study based on observational data over China found rainfall intensity is predominantly controlled by variations in PW with CAPE playing a secondary role, especially at large values of CAPE (Dong et al., 2019). Similar observational analysis would be useful to help explore the relationships over the Amazon.

Our work further highlights how atmospheric circulation responses modify the response of precipitation to land cover change. Luo et al. (2022) found that 7 out of 11 CMIP6 models simulated a reduction in MFC in response to Amazon deforestation, which is in line with the results from our model. In the dry season, we find that lower ET drives surface warming and drying, resulting in a reduction in CAPE (up to −25 J·kg<sup>−1</sup>), which further causes reduced precipitation, upper atmosphere cooling and reduced incoming wind that drives overall reductions in MFC. The high sensitivity of precipitation to deforestation in our study is caused by a combination of deforestation driving reduced atmospheric moisture convergence that magnifies reductions in atmospheric moisture, combined with reduced precipitation efficiency largely driven by reductions in atmospheric moisture. Climate models disagree on the response of atmospheric moisture convergence to deforestation in the Amazon due to divergent responses of ET and atmospheric moisture convergence to deforestation across the models (Luo et al., 2022); understanding this disagreement should be a priority for future research.

In this study, we focus on the atmospheric branch of the water cycle, specifically how deforestation alters evapotranspiration, atmospheric moisture transport, and precipitation. Deforestation also impacts river runoff through changes to precipitation and ET. Deforestation reduces ET which acts to increase river runoff (Sterling et al., 2013). Previous studies have suggested Amazon deforestation increases runoff via this effect (Guimberteau et al., 2017; Levy et al., 2018). However, deforestation also reduces rainfall which acts to reduce runoff, but most previous studies ignore this interaction. Stickler et al. (2013) found that deforestation in the eastern Amazon increased runoff by 10%–12% when only effects on ET were included, but this swapped to a reduction in runoff of 6%–36% when effects on rainfall were also considered. We estimate deforestation has reduced dry season land storage and runoff in Mato Grosso and Rondônia by 5% (Figure 3), because deforestation results in larger reductions in precipitation compared to ET. Our work confirms the importance of accounting for deforestation-driven changes in rainfall when calculating impacts of deforestation on the regional water balance. Crucially we find that reductions in rainfall are large enough to counteract increased ET, meaning deforestation could result

in reduced rather than increased river runoff. Deforestation may also lead to soil compaction and reduced ground water recharge that would further reduce dry season river flows (Chagas et al., 2022). Long-term monitoring of all components of the water balance in the Amazon is needed to fully understand and track such changes (Heerspink et al., 2020).

Moreover, the discrepancy between simulated ET and MODIS-derived ET, particularly the underestimation in the dry season and the larger differences in the wet season (Figure S1b in Supporting Information S1), likely arises from a combination of WRF biases and uncertainties in the MODIS product. The MODIS ET product primarily relies on other MODIS data sets (e.g., LAI, FPAR etc.), and uncertainties from these inputs can introduce biases in ET estimates that are difficult to detect (Mu et al., 2021; Ruhoff et al., 2012). Despite these uncertainties, MODIS ET was one of the better performing satellite ET data sets for the Amazon, with better correspondence with catchment-balance ET including capturing spatial and seasonal patterns of variation (Baker et al., 2021). The Noah-MP scheme also has ET biases due to issues representing the carbon partitioning into shoot and root, root dynamics, and the feedbacks to photosynthesis (Ma et al., 2017). Given these uncertainties, our study focuses on differences between model simulations rather than relying on MODIS as an absolute benchmark. However, addressing challenges in estimating Amazon ET requires further investigations such as combining MODIS with other ET data sets and enhancing soil-vegetation interactions in Noah-MP, particularly for deep-rooted forests, may reduce model biases in ET.

### 3.3. Implications

Our results suggest that land cover change in Mato Grosso and Rondônia over the period 2002–2015 has reduced regional mean precipitation during the dry season by more than 5%. This reduction in dry season precipitation will have resulted in widespread negative impacts including increased riverflow seasonality (Wang et al., 2024), reduced energy generation from hydropower (Stickler et al., 2013), reduced agricultural yields (Leite-Filho et al., 2021), and increased probability of fire (Butt et al., 2022; Fonseca et al., 2019). Agricultural expansion in the southern Amazon and Cerrado biomes coincides with regions experiencing rapid warming and drying (Marengo et al., 2022). Future deforestation combined with climate change could result in further reductions in precipitation (Brito et al., 2023; Lemes et al., 2023; Sampaio et al., 2021) which would exacerbate these impacts. Our analysis further confirms the negative impacts of deforestation in Mato Grosso and Rondônia and provides evidence to support a comprehensive forest conservation strategy including well managed protected areas and Indigenous Lands (Soares-Filho et al., 2023), robust environmental protection strategies and continuing law enforcement (Gatti et al., 2023).

### 4. Conclusions

We examined the biophysical effects of forest cover change on precipitation and the terrestrial water balance in the southern Amazon. Unlike many previous works that focused on idealized land cover scenarios, we simulated the impacts of recent vegetation changes using land surface properties prescribed by satellite. We studied the impacts of forest loss in Mato Grosso and Rondônia, two states in the southern Brazilian Amazon that have experienced extensive deforestation. We used a regional climate model with embedded water vapor tracers that allowed us to separate local and non-local sources of moisture. Over the period 2002 to 2015, mean forest cover loss of 3.2% caused, on average, a 5.4% reduction in the simulated dry season mean precipitation. This shows that recent forest cover change in the southern Amazon has led to considerable reductions in dry season precipitation, which is in line with recent observational studies (Smith, Baker, & Spracklen et al., 2023; Smith, Robertson, et al., 2023).

We analyzed the effects of forest cover change on the different components of the moisture budget. Forest cover change causes a  $4.2 \text{ mm-month}^{-1}$  reduction in dry season mean evapotranspiration and a  $2.2 \text{ mm-month}^{-1}$  reduction in dry season mean flow convergence. The reduction in non-local moisture amplifies the impacts of reduced moisture recycling. Therefore studies that assume precipitation decreases proportionally to the reduction in evapotranspiration are likely to underestimate the impacts of deforestation on precipitation. Results from the tagged water vapor tracers show that 76.9% of the reduction in dry season mean precipitation resulted from a reduction in non-local water vapor and 23.1% resulted from a reduction in local evaporated water vapor. Our results suggest that changes in local moisture recycling lead to atmospheric responses that amplify the precipitation reduction due to forest loss.

Through the analysis of the surface energy balance and vertical atmospheric profiles, we determined the mechanisms for the simulated changes in the water vapor cycle. In the dry season, deforestation results in reduced ET and associated latent heat, resulting in surface warming and drying. Reductions in lower troposphere specific humidity reduced CAPE, resulting in reduced convection and precipitation. This reduction in precipitation efficiency was responsible for 84.5% of the precipitation reduction in the dry season. Cooling of the upper troposphere led to reductions in upper level moisture inflow. Our study highlights the importance of atmospheric responses to land cover change, resulting in non-linear responses of precipitation, which are not considered by many studies.

Deforestation led to reduction in mean precipitation efficiency. However, under high-moisture regimes, forest loss led to increased daily precipitation rates, which confirms recent research suggesting deforestation-driven intensification of storms (Taylor et al., 2022). By analyzing precipitation changes at different time scales, we found that the changes in precipitation efficiency at a seasonal scale are driven by variations in atmospheric moisture content, which underscores the importance of considering multiple time scales when analyzing changes in the water vapor cycle.

Overall, our results suggest that recent deforestation in Mato Grosso and Rondônia has resulted in reductions in dry season precipitation, dominated by changes in convection and precipitation efficiency amplifying changes in moisture recycling. Reductions in dry season precipitation will have wide-ranging negative impacts, including on agriculture, local livelihoods and natural ecosystems. Our work highlights the importance of forest protection and sustainable forest management to maintain regional rainfall patterns.

### Conflict of Interest

The authors declare no conflicts of interest relevant to this study.

### Data Availability Statement

The WRF simulations are available at <https://www2.mmm.ucar.edu/wrf/>. The water vapor tracers and source code are available at <https://github.com/damianinsua/WRF-WVTs>. The land cover type data are available at <https://doi.org/10.5067/MODIS/MCD12C1.006>. The snow-free albedo data are available at <https://doi.org/10.5067/MODIS/MCD43GF.006>. The leaf area index data are available at <http://globalchange.bnu.edu.cn/research/laiv6>. The green vegetation fraction data are available at <http://www.glass.umd.edu/FAPAR/MODIS/0.05D/>. The roughness length data are available at <https://doi.org/10.5281/zenodo.4662935>. The NCEP FNL Operational Model Global Tropospheric Analyses data are available at <https://doi.org/10.5065/D6M043C6>. The observed evapotranspiration data are available at <https://lpdaac.usgs.gov/products/mod16a2v061>. The observed precipitation data are available at [https://disc.gsfc.nasa.gov/datasets/TRMM\\_3B42\\_Daily\\_7/summary](https://disc.gsfc.nasa.gov/datasets/TRMM_3B42_Daily_7/summary). The observed deforestation data PRODES are available at <http://www.obt.inpe.br/OBT/assuntos/programas/amazonia/prodes>. Source data are provided at <https://zenodo.org/records/15272568>.

### References

- Alkama, R., & Cescatti, A. (2016). Biophysical climate impacts of recent changes in global forest cover. *Science*, 351(6273), 600–604. <https://doi.org/10.1126/science.aac8083>
- Almeida, C. A., Maurano, L. E. P., Valeriano, D. M., Câmara, G., Vinhas, L., Motta, M., et al. (2022). Metodologia utilizada nos sistemas PRODES e DETER - 2ª edição (atualizada) [Dataset]. *Coordenação-Geral de Observação da Terra*. Retrieved from <http://www.obt.inpe.br/OBT/assuntos/programas/amazonia/prodes>
- Alves, L. M., Marengo, J. A., Fu, R., & Bombardi, R. J. (2017). Sensitivity of Amazon regional climate to deforestation. *American Journal of Climate Change*, 6(1), 75–98. <https://doi.org/10.4236/ajcc.2017.61005>
- Alves de Oliveira, B. F., Bottino, M. J., Nobre, P., & Nobre, C. A. (2021). Deforestation and climate change are projected to increase heat stress risk in the Brazilian Amazon. *Communications Earth & Environment*, 2(1), 207. <https://doi.org/10.1038/s43247-021-00275-8>
- Artaxo, P., Hansson, H.-C., Andreae, M. O., Bäck, J., Alves, E. G., Barbosa, H. M. J., et al. (2022). Tropical and boreal forest – Atmosphere interactions: A review. *Chemical and Physical Meteorology*, 74(1), 24–163. <https://doi.org/10.16993/tellusb.34>
- Bagley, J., Desai, A., Harding, K., Snyder, P., & Foley, J. (2014). Drought and deforestation: Has land cover change influenced recent precipitation extremes in the Amazon? *Journal of Climate*, 27(1), 345–361. <https://doi.org/10.1175/JCLI-D-12-00369.1>
- Baker, J. C., Garcia-Carreras, L., Gloor, M., Marsham, J. H., Buermann, W., da Rocha, H. R., et al. (2021). Evapotranspiration in the Amazon: Spatial patterns, seasonality, and recent trends in observations, reanalysis, and climate models. *Hydrology and Earth System Sciences*, 25(4), 2279–2300. <https://doi.org/10.5194/hess-25-2279-2021>
- Baker, J. C., & Spracklen, D. V. (2019). Climate benefits of intact Amazon forests and the biophysical consequences of disturbance. *Frontiers in Forests and Global Change*, 2, 47. <https://doi.org/10.3389/ffgc.2019.00047>
- Baker, J. C. A., & Spracklen, D. V. (2022). Divergent representation of precipitation recycling in the Amazon and the Congo in CMIP6 models. *Geophysical Research Letters*, 49(10), e2021GL095136. <https://doi.org/10.1029/2021GL095136>

### Acknowledgments

This research is supported by the National Natural Science Foundation of China (Grants 42130602 and 42375115), the Jiangsu Collaborative Innovation Center for Climate Change, and the Frontiers Science Center for Critical Earth Material Cycling of Nanjing University. DVS acknowledges support from the European Research Council (ERC) under the European Union's Horizon 2020 research and innovation programme (DECAF project, Grant agreement No. 771492), the Newton Fund through the Met Office Climate Science for Service Partnership Brazil (CSSP Brazil) and the Natural Environment Research Council (NE/Z00005X/1). J.G. acknowledges support from the National Natural Science Foundation of China (42375115).

- Baudena, M., Tuinenburg, O. A., Ferdinand, P. A., & Staal, A. (2021). Effects of land-use change in the Amazon on precipitation are likely underestimated. *Global Change Biology*, 27(21), 5580–5587. <https://doi.org/10.1111/gcb.15810>
- Borma, L. S., Costa, M. H., da Rocha, H. R., Arieira, J., Nascimento, N. C. C., Jaramillo-Giraldo, C., et al. (2022). Beyond carbon: The contributions of South American tropical humid and subhumid forests to ecosystem services. *Reviews of Geophysics*, 60(4), e2021RG000766. <https://doi.org/10.1029/2021RG000766>
- Bright, R. M., Davin, E., O'Halloran, T., Pongratz, J., Zhao, K., & Cescatti, A. (2017). Local temperature response to land cover and management change driven by non-radiative processes. *Nature Climate Change*, 7(4), 296–302. <https://doi.org/10.1038/nclimate3250>
- Brito, A. L., Veiga, J. A. P., Correia, F. S., Michiles, A. A., Capistrano, V. B., Chou, S. C., et al. (2023). Impacts of increasing greenhouse gas concentrations and deforestation on extreme rainfall events in the Amazon basin: A multi-model ensemble-based study. *International Journal of Climatology*, 43(12), 5512–5535. <https://doi.org/10.1002/joc.8158>
- Butt, E. W., Baker, J. C., Bezerra, F. G. S., von Randow, C., Aguiar, A. P., & Spracklen, D. V. (2023). Amazon deforestation causes strong regional warming. *Proceedings of the National Academy of Sciences*, 120(45), e2309123120. <https://doi.org/10.1073/pnas.2309123120>
- Butt, E. W., Conibear, L., Smith, C., Baker, J. C., Rigby, R., Knote, C., & Spracklen, D. V. (2022). Achieving Brazil's deforestation target will reduce fire and deliver air quality and public health benefits. *Earth's Future*, 10(12), e2022EF003048. <https://doi.org/10.1029/2022EF003048>
- Chagas, V. B. P., Chaffe, P. L. B., & Blöschl, G. (2022). Climate and land management accelerate the Brazilian water cycle. *Nature Communications*, 13(1), 5136. <https://doi.org/10.1038/s41467-022-32580-x>
- Chug, D., Dominguez, F., & Yang, Z. (2022). The Amazon and La Plata river basins as moisture sources of South America: Climatology and intraseasonal variability. *Journal of Geophysical Research: Atmospheres*, 127(12), e2021JD035455. <https://doi.org/10.1029/2021JD035455>
- Commar, L. F. S. A., Abrahão, G. M., & Costa, M. H. (2023). A possible deforestation-induced synoptic-scale circulation that delays the rainy season onset in Amazonia. *Environmental Research Letters*, 18(4), 044041. <https://doi.org/10.1088/1748-9326/acc95f>
- Csillik, O., Keller, M., Longo, M., Ferraz, A., Rangel Pinagé, E., Görgens, E. B., et al. (2024). A large net carbon loss attributed to anthropogenic and natural disturbances in the Amazon Arc of Deforestation. *Proceedings of the National Academy of Sciences*, 121(33), e2310157121. <https://doi.org/10.1073/pnas.2310157121>
- Davin, E. L., de Noblet-Ducoudré, N., & Friedlingstein, P. (2007). Impact of land cover change on surface climate: Relevance of the radiative forcing concept. *Geophysical Research Letters*, 34(13), L13702. <https://doi.org/10.1029/2007GL029678>
- De Sales, F., Santiago, T., Biggs, T. W., Mullan, K., Sills, E. O., & Monteverde, C. (2020). Impacts of protected area deforestation on dry-season regional climate in the Brazilian Amazon. *Journal of Geophysical Research: Atmospheres*, 125(16), e2020JD033048. <https://doi.org/10.1029/2020JD033048>
- Dominguez, F., Eiras-Barca, J., Yang, Z., Bock, D., Nieto, R., & Gimeno, L. (2022). Amazonian moisture recycling revisited using WRF with water vapour tracers. *Journal of Geophysical Research: Atmospheres*, 127(4), e2021JD035259. <https://doi.org/10.1029/2021JD035259>
- Dong, W., Lin, Y., Wright, J. S., Xie, Y., Yin, X., & Guo, J. (2019). Precipitable water and CAPE dependence of rainfall intensities in China. *Climate Dynamics*, 52(5–6), 3357–3368. <https://doi.org/10.1007/s00382-018-4327-8>
- Drumond, A., Marengo, J., Ambrizzi, T., Nieto, R., Moreira, L., & Gimeno, L. (2014). The role of the Amazon basin moisture in the atmospheric branch of the hydrological cycle: A Lagrangian analysis. *Hydrology and Earth System Sciences*, 18(7), 2577–2598. <https://doi.org/10.5194/hess-18-2577-2014>
- Duku, C., & Hein, L. (2023). Assessing the impacts of past and ongoing deforestation on rainfall patterns in South America. *Global Change Biology*, 29(18), 5292–5303. <https://doi.org/10.1111/gcb.16856>
- Duveiller, G., Caporaso, L., Abad-Viñas, R., Perugini, L., Grassi, G., Arneth, A., & Cescatti, A. (2020). Local biophysical effects of land use and land cover change: Towards an assessment tool for policy makers. *Land Use Policy*, 91, 104382. <https://doi.org/10.1016/j.landusepol.2019.104382>
- Ellison, D., Morris, C. E., Locatelli, B., Sheil, D., Cohen, J., Murdiyarto, D., et al. (2017). Trees, forests and water: Cool insights for a hot world. *Global Environmental Change*, 43, 51–61. <https://doi.org/10.1016/j.gloenvcha.2017.01.002>
- Fonseca, M. G., Alves, L. M., Aguiar, A. P. D., Arai, E., Anderson, L. O., Rosan, T. M., et al. (2019). Effects of climate and land-use change scenarios on fire probability during the 21st century in the Brazilian Amazon. *Global Change Biology*, 25(9), 2931–2946. <https://doi.org/10.1111/gcb.14709>
- Friedl, M., & Sulla-Menashe, D. (2015). MCD12C1 MODIS/Terra+Aqua Land Cover Type Yearly L3 Global 0.05Deg CMG V006 [Dataset]. *NASA EOSDIS Land Processes DAAC*. <https://doi.org/10.5067/MODIS/MCD12C1.006>
- García-Carreras, L., & Parker, D. J. (2011). How does local tropical deforestation affect rainfall? *Geophysical Research Letters*, 38(19), L19802. <https://doi.org/10.1029/2011GL049099>
- Gatti, L. V., Cunha, C. L., Marani, L., Cassol, H. L., Messias, C. G., Arai, E., et al. (2023). Increased Amazon carbon emissions mainly from decline in law enforcement. *Nature*, 621(7978), 318–323. <https://doi.org/10.1038/s41586-023-06390-0>
- Ge, J., Pitman, A. J., Guo, W. D., Zan, B. L., & Fu, C. B. (2020). Impact of revegetation of the Loess Plateau of China on the regional growing season water balance. *Hydrology and Earth System Sciences*, 24(2), 515–533. <https://doi.org/10.5194/hess-24-515-2020>
- Gomes, H. B., Lemos da Silva, M. C., Barbosa, H. D. M. J., Ambrizzi, T., Baltaci, H., Gomes, H. B., et al. (2022). WRF sensitivity for seasonal climate simulations of precipitation fields on the CORDEX South America domain. *Atmosphere*, 13(1), 107. <https://doi.org/10.3390/atmos13010107>
- Guimberteau, M., Ciais, P., Ducharme, A., Boisier, J. P., Dutra Aguiar, A. P., Biemans, H., et al. (2017). Impacts of future deforestation and climate change on the hydrology of the Amazon Basin: A multi-model analysis with a new set of land-cover change scenarios. *Hydrology and Earth System*, 21(3), 1455–1475. <https://doi.org/10.5194/hess-21-1455-2017>
- Heerspink, B. P., Kendall, A. D., Coe, M. T., & Hyndman, D. W. (2020). Trends in streamflow, evapotranspiration, and groundwater storage across the Amazon Basin linked to changing precipitation and land cover. *Journal of Hydrology: Regional Studies*, 32, 100755. <https://doi.org/10.1016/j.ejrh.2020.100755>
- Heinrich, V. H. A., Dalagnol, R., Cassol, H. L. G., Rosan, T. M., de Almeida, C. T., Silva Junior, C. H. L., et al. (2021). Large carbon sink potential of Amazonian secondary forests to mitigate climate change. *Nature Communications*, 12, 4–6. <https://doi.org/10.1038/s41467-021-22050-1>
- Hong, S. Y., & Lim, J. (2006). The WRF single-moment 6-class microphysics scheme (WSM6). *Journal of the Korean Meteorological Society*, 42, 129–151.
- Hong, S. Y., Noh, Y., & Dudhia, J. (2006). A new vertical diffusion package with an explicit treatment of entrainment processes. *Monthly Weather Review*, 134(9), 2318–2341. <https://doi.org/10.1175/MWR3199.1>
- Huffman, G. J., Bolvin, D. T., Nelkin, E. J., & Adler, R. F. (2016). In A. Savtchenko (Ed.), *TRMM (TMPA) Precipitation L3 1 day 0.25 degree × 0.25 degree V7*. Goddard Earth Sciences Data and Information Services Center (GES DISC). <https://doi.org/10.5067/TRMM/TMPA/DAY/7>

- Iacono, M. J., Delamere, J. S., Mlawer, E. J., Shephard, M. W., Clough, S. A., & Collins, W. D. (2008). Radiative forcing by long-lived greenhouse gases: Calculations with the AER radiative transfer models. *Journal of Geophysical Research*, *113*(D13), D13103. <https://doi.org/10.1029/2008JD009944>
- Insua-Costa, D., & Miguez-Macho, G. (2018). A new moisture tagging capability in the Weather Research and Forecasting model: Formulation, validation and application to the 2014 Great Lake-effect snowstorm. *Earth System Dynamics*, *9*(1), 167–185. <https://doi.org/10.5194/esd-9-167-2018>
- Jenkins, C. N., Pimm, S. L., & Joppa, L. N. (2013). Global patterns of terrestrial vertebrate diversity and conservation. *Proceedings of the National Academy of Sciences*, *110*(28), E2602–E2610. <https://doi.org/10.1073/pnas.1302251110>
- Kain, J. S. (2004). The Kain-Fritsch convective parameterization: An update. *Journal of Applied Meteorology*, *43*(1), 170–181. [https://doi.org/10.1175/1520-0450\(2004\)043<0170:TKCPAU>2.0.CO;2](https://doi.org/10.1175/1520-0450(2004)043<0170:TKCPAU>2.0.CO;2)
- Khanna, J., Medvigy, D., Fueglistaler, S., & Walko, R. (2017). Regional dry-season climate changes due to three decades of Amazonian deforestation. *Nature Climate Change*, *7*(3), 200–204. <https://doi.org/10.1038/nclimate3226>
- Kumar, A., Chen, F., Barlage, M., Ek, M. B., & Niyogi, D. (2014). Assessing impacts of integrating MODIS vegetation data in the Weather Research and Forecasting (WRF) model coupled to two different canopy-resistance approaches. *Journal of Applied Meteorology and Climatology*, *53*(6), 1362–1380. <https://doi.org/10.1175/JAMC-D-13-0247.1>
- Langenbrunner, B., Pritchard, M. S., Kooperman, G. J., & Randerson, J. T. (2019). Why does Amazon precipitation decrease when tropical forests respond to increasing CO<sub>2</sub>? *Earth's Future*, *7*(4), 450–468. <https://doi.org/10.1029/2018EF001026>
- Lawrence, D., Coe, M., Walker, W., Verchot, L., & VandeCar, K. (2022). The unseen effects of deforestation: Biophysical effects on climate. *Frontiers in Forests and Global Change*, *5*, 756115. <https://doi.org/10.3389/ffgc.2022.756115>
- Leite-Filho, A. T., Costa, M. H., & Fu, R. (2019). The southern Amazon rainy season: The role of deforestation and its interactions with large-scale mechanisms. *International Journal of Climatology*, *40*(4), 2328–2341. <https://doi.org/10.1002/joc.6335>
- Leite-Filho, A. T., Soares-Filho, B. S., Davis, J. L., Abrahão, G. M., & Börner, J. (2021). Deforestation reduces rainfall and agricultural revenues in the Brazilian Amazon. *Nature Communications*, *12*(1), 2591. <https://doi.org/10.1038/s41467-021-22840-7>
- Lemes, M. R., Sampaio, G., Garcia-Carreras, L., Fisch, G., Alves, L. M., Bassett, R., et al. (2023). Impacts on South America moisture transport under Amazon deforestation and 2°C global warming. *Science of the Total Environment*, *905*, 167407. <https://doi.org/10.1016/j.scitotenv.2023.167407>
- Levy, M. C., Lopes, A. V., Cohn, A., Larsen, L. G., & Thompson, S. E. (2018). Land use change increases streamflow across the arc of deforestation in Brazil. *Geophysical Research Letters*, *45*(8), 3520–3530. <https://doi.org/10.1002/2017GL076526>
- Li, Y., Brando, P. M., Morton, D. C., Lawrence, D. M., Yang, H., & Randerson, J. T. (2022). Deforestation-induced climate change reduces carbon storage in remaining tropical forests. *Nature Communications*, *13*(1), 1964. <https://doi.org/10.1038/s41467-022-29601-0>
- Lima, A. L., Veiga, J. A., Brito, A. L., & Correia, F. W. (2023). Effects of deforestation at different spatial scales on the climate of the Amazon basin. *Climate Research*, *91*, 21–46. <https://doi.org/10.3354/cr01717>
- Liu, Y., Ge, J., Guo, W., Cao, Y., Chen, C., Luo, X., et al. (2023). Revisiting biophysical impacts of greening on precipitation over the Loess Plateau of China using WRF with water vapour tracers. *Geophysical Research Letters*, *50*(8), e2023GL102809. <https://doi.org/10.1029/2023GL102809>
- Liu, Y., Guo, W., Huang, H., Ge, J., & Qiu, B. (2021). Global aerodynamic parameters in 1982–2017 based on GIMMS LAI [Dataset]. In *Estimating global aerodynamic parameters in 1982–2017 using remote-sensing data and a turbulent transfer model* (Vol. 260, p. 112428). Zenodo. <https://doi.org/10.5281/zenodo.4662935>
- Liu, Z. Y., Notaro, M., Kutzbach, J., & Liu, N. (2006). Assessing global vegetation-climate feedbacks from observations. *Journal of Climate*, *19*(5), 787–814. <https://doi.org/10.1175/JCLI3658.1>
- Luo, X., Ge, J., Guo, W. D., Fan, L., Chen, C. R., Liu, Y., & Yang, L. M. (2022). The biophysical impacts of deforestation on precipitation: Results from the CMIP6 model intercomparison. *Journal of Climate*, *35*(11), 3293–3311. <https://doi.org/10.1175/JCLI-D-21-0689.1>
- Ma, N., Niu, G. Y., Xia, Y., Cai, X., Zhang, Y., Ma, Y., & Fang, Y. (2017). A systematic evaluation of Noah-MP in simulating land-atmosphere energy, water, and carbon exchanges over the continental United States. *Journal of Geophysical Research: Atmospheres*, *122*(22), 12245–12268. <https://doi.org/10.1002/2017JD027597>
- Makarieva, A. M., Nefiodov, A. V., Nobre, A. D., Baudena, M., Bardi, U., Sheil, D., et al. (2023). The role of ecosystem transpiration in creating alternate moisture regimes by influencing atmospheric moisture convergence. *Global Change Biology*, *29*(9), 2536–2556. <https://doi.org/10.1111/gcb.16644>
- Marengo, J. A., Jimenez, J. C., Espinoza, J. C., Cunha, A. P., & Aragão, L. E. (2022). Increased climate pressure on the agricultural frontier in the Eastern Amazonia–Cerrado transition zone. *Scientific Reports*, *12*(1), 457. <https://doi.org/10.1038/s41598-021-04241-4>
- Marengo, J. A., Souza, C. M., Jr., Thonicke, K., Burton, C., Halladay, K., Betts, R. A., et al. (2018). Changes in climate and land use over the Amazon region: Current and future variability and trends. *Frontiers in Earth Science*, *6*, 228. <https://doi.org/10.3389/feart.2018.00228>
- Mu, Y., Biggs, T. W., & De Sales, F. (2021). Forests mitigate drought in an agricultural region of the Brazilian Amazon: Atmospheric moisture tracking to identify critical source areas. *Geophysical Research Letters*, *48*(5), e2020GL091380. <https://doi.org/10.1029/2020GL091380>
- National Centers for Environmental Prediction/National Weather Service/NOAA/U.S. Department of Commerce. (2000). NCEP FNL Operational Model Global Tropospheric Analyses, continuing from July 1999 [Dataset]. *Research Data Archive at the National Center for Atmospheric Research, Computational and Information Systems Laboratory*. <https://doi.org/10.5065/D6M043C6>
- Niu, G. Y., Yang, Z. L., Mitchell, K. E., Chen, F., Ek, M. B., Barlage, M., et al. (2011). The community Noah land surface model with multi-parameterization options (Noah-MP): 1. Model description and evaluation with local-scale measurements. *Journal of Geophysical Research*, *116*(D12), D12109. <https://doi.org/10.1029/2010JD015139>
- Piao, S. L., Wang, X. H., Park, T. J., Chen, C., Lian, X., He, Y., et al. (2020). Characteristics, drivers and feedbacks of global greening. *Nature Reviews Earth & Environment*, *1*, 14–27. <https://doi.org/10.1038/s43017-019-0001-x>
- Qin, Y., Xiao, X., Dong, J., Zhang, Y., Wu, X., Shimabukuro, Y., et al. (2019). Improved estimates of forest cover and loss in the Brazilian Amazon in 2000–2017. *Nature Sustainability*, *2*(8), 764–772. <https://doi.org/10.1038/s41893-019-0336-9>
- Ruhoff, A. L., Collischonn, W., Paz, A. R., Rocha, H. R., Aragao, L. E., Malhi, Y., et al. (2012). Validation of the global evapotranspiration algorithm (MOD16) in two contrasting tropical land cover types. *Remote Sensing and Hydrology*, *352*, 128–131.
- Ruiz-Vásquez, M., Arias, P. A., Martínez, J. A., & Espinoza, J. C. (2020). Effects of Amazon basin deforestation on regional atmospheric circulation and water vapour transport towards tropical South America. *Climate Dynamics*, *54*(9–10), 4169–4189. <https://doi.org/10.1007/s00382-020-05223-4>
- Running, S., Mu, Q., & Zhao, M. (2021). *MODIS/Terra Net Evapotranspiration 8-Day L4 Global 500m SIN Grid V061*. Distributed by NASA EOSDIS Land Processes Distributed Active Archive Center. <https://doi.org/10.5067/MODIS/MOD16A2.061>

- Sampaio, G., Shimizu, M. H., Guimarães-Júnior, C. A., Alexandre, F., Guatura, M., Cardoso, M., et al. (2021). CO<sub>2</sub> physiological effect can cause rainfall decrease as strong as large-scale deforestation in the Amazon. *Biogeosciences*, 18(8), 2511–2525. <https://doi.org/10.5194/bg-18-2511-2021>
- Schaaf, C. (2019). MODIS/Terra+Aqua BRDF/Albedo Gap-Filled Snow-Free Daily L3 Global 30ArcSec CMG V006 [Dataset]. *NASA EOSDIS Land Processes DAAC*. <https://doi.org/10.5067/MODIS/MCD43GF006>
- Seager, R., Ting, M., Held, I., Kushnir, Y., Lu, J., Vecchi, G., et al. (2007). Model projections of an imminent transition to a more arid climate in southwestern North America. *Science*, 316(5828), 181–184. <https://doi.org/10.1126/science.1139601>
- Sierra, J. P., Espinoza, J. C., Junquas, C., Wongchuig, S., Polcher, J., Moron, V., et al. (2023). Impacts of land-surface heterogeneities and Amazonian deforestation on the wet season onset in southern Amazon. *Climate Dynamics*, 61(9), 4867–4898. <https://doi.org/10.1007/s00382-023-06835-2>
- Smith, C., Baker, J. C. A., & Spracklen, D. V. (2023). Tropical deforestation causes large reductions in observed precipitation. *Nature*, 615(7951), 270–275. <https://doi.org/10.1038/s41586-022-05690-1>
- Smith, C., Robertson, E., Chadwick, R., Kelley, D. I., Argles, A. P., Coelho, C. A., et al. (2023). Observed and simulated local climate responses to tropical deforestation. *Environmental Research Letters*, 18(10), 104004. <https://doi.org/10.1088/1748-9326/acfd0a>
- Soares-Filho, B. S., Oliveira, U., Ferreira, M. N., Marques, F. F. C., de Oliveira, A. R., Silva, F. R., & Börner, J. (2023). Contribution of the Amazon protected areas program to forest conservation. *Biological Conservation*, 279, 109928. <https://doi.org/10.1016/j.biocon.2023.109928>
- Spera, S. A., Winter, J. M., & Partridge, T. F. (2020). Brazilian maize yields negatively affected by climate after land clearing. *Nature Sustainability*, 3(10), 845–852. <https://doi.org/10.1038/s41893-020-0560-3>
- Spracklen, D. V., Baker, J. C. A., Garcia-Carreras, L., & Marsham, J. H. (2018). The effects of tropical vegetation on rainfall. *Annual Review of Environment and Resources*, 43(1), 193–218. <https://doi.org/10.1146/annurev-environ-102017-030136>
- Spracklen, D. V., & Garcia-Carreras, L. (2015). The impact of Amazonian deforestation on Amazon basin rainfall. *Geophysical Research Letters*, 42, 9546–9552. <https://doi.org/10.1002/2015GL066063>
- Staal, A., Tuinenburg, O. A., Bosmans, J. H., Holmgren, M., van Nes, E. H., Scheffer, M., et al. (2018). Forest-rainfall cascades buffer against drought across the Amazon. *Nature Climate Change*, 8(6), 539–543. <https://doi.org/10.1038/s41558-018-0177-y>
- Sterling, S., Ducharme, A., & Polcher, J. (2013). The impact of global land-cover change on the terrestrial water cycle. *Nature Climate Change*, 3(4), 385–390. <https://doi.org/10.1038/nclimate1690>
- Steyaert, L. T., & Knox, R. G. (2008). Reconstructed historical land cover and biophysical parameters for studies of land-atmosphere interactions within the eastern United States. *Journal of Geophysical Research*, 113(D2), D02101. <https://doi.org/10.1029/2006JD008277>
- Stickler, C. M., Coe, M. T., Costa, M. H., Nepstad, D. C., McGrath, D. G., Dias, L. C., et al. (2013). Dependence of hydropower energy generation on forests in the Amazon Basin at local and regional scales. *Proceedings of the National Academy of Sciences*, 110(23), 9601–9606. <https://doi.org/10.1073/pnas.1215331110>
- Swann, A. L., Longo, M., Knox, R. G., Lee, E., & Moorcroft, P. R. (2015). Future deforestation in the Amazon and consequences for South American climate. *Agricultural and Forest Meteorology*, 214, 12–24. <https://doi.org/10.1016/j.agrformet.2015.07.006>
- Tai, S. L., Feng, Z., Marquis, J., & Fast, J. (2024). Characterizing wet season precipitation in the central Amazon using a mesoscale convective system tracking algorithm. *Journal of Geophysical Research: Atmospheres*, 129(19), e2024JD041004. <https://doi.org/10.1029/2024JD041004>
- Taylor, C. M., Klein, C., Parker, D. J., Gerard, F., Semeena, V. S., Barton, E. J., & Harris, B. L. (2022). “Late-stage” deforestation enhances storm trends in coastal West Africa. *Proceedings of the National Academy of Sciences*, 119(2), e2109285119. <https://doi.org/10.1073/pnas.2109285119>
- Van der Ent, R. J., Savenije, H. H., Schaeffli, B., & Steele-Dunne, S. C. (2010). Origin and fate of atmospheric moisture over continents. *Water Resources Research*, 46(9), W09525. <https://doi.org/10.1029/2010WR009127>
- Wang, H., Liu, J., Klaar, M., Chen, A., Gudmundsson, L., & Holden, J. (2024). Anthropogenic climate change has influenced global river flow seasonality. *Science*, 383(6686), 1009–1014. <https://doi.org/10.1126/science.ad9501>
- Wang, Y., Ziv, G., Adami, M., Almeida, C. A., Antunes, J. F. G., Coutinho, A. C., et al. (2020). Upturn in secondary forest clearing buffers primary forest loss in the Brazilian Amazon. *Nature Sustainability*, 3(4), 290–295. <https://doi.org/10.1038/s41893-019-0470-4>
- Wright, J. S., Fu, R., Worden, J. R., Chakraborty, S., Clinton, N. E., Risi, C., et al. (2017). Rainforest-initiated wet season onset over the southern Amazon. *Proceedings of the National Academy of Sciences*, 114(32), 8481–8486. <https://doi.org/10.1073/pnas.1621516114>
- Xiao, Z. Q., Liang, S. L., & Sun, R. (2018). Evaluation of three long time series for global fraction of absorbed photosynthetically active radiation (FAPAR) products. *IEEE Transactions on Geoscience and Remote Sensing*, 56(9), 5509–5524. <https://doi.org/10.1109/TGRS.2018.2818929>
- Xiao, Z. Q., Liang, S. L., Sun, R., Wang, J. D., & Jiang, B. (2015). Estimating the fraction of absorbed photosynthetically active radiation from the MODIS data based GLASS leaf area index product. *Remote Sensing of Environment*, 171, 105–117. <https://doi.org/10.1016/j.rse.2015.10.016>
- Xu, X., Zhang, X., Riley, W. J., Xue, Y., Nobre, C. A., Lovejoy, T. E., & Jia, G. (2022). Deforestation triggering irreversible transition in Amazon hydrological cycle. *Environmental Research Letters*, 17(3), 034037. <https://doi.org/10.1088/1748-9326/ac4c1d>
- Yuan, H., Dai, Y., & Li, S. (2020). Reprocessed MODIS Version 6 Leaf Area Index data sets for land surface and climate modelling [Dataset]. *Sun Yat-sun University*. <http://globalchange.bnu.edu.cn/research/laiv6>
- Yuan, H., Dai, Y. J., Xiao, Z. Q., Ji, D. Y., & Shangguan, W. (2011). Reprocessing the MODIS Leaf Area Index products for land surface and climate modelling. *Remote Sensing of Environment*, 115(5), 1171–1187. <https://doi.org/10.1016/j.rse.2011.01.001>
- Zemp, D. C., Schleussner, C. F., Barbosa, H. M. J., Van der Ent, R. J., Donges, J. F., Heinke, J., et al. (2014). On the importance of cascading moisture recycling in South America. *Atmospheric Chemistry and Physics*, 14(23), 13337–13359. <https://doi.org/10.5194/acp-14-13337-2014>

## References From the Supporting Information

- Chen, C. R., Ge, J., Guo, W. D., Cao, Y. P., Liu, Y., Luo, X., & Yang, L. M. (2022). The biophysical impacts of idealized afforestation on surface temperature in China: Local and nonlocal effects. *Journal of Climate*, 35(23), 7833–7852. <https://doi.org/10.1175/JCLI-D-22-0144.1>
- Chen, L., & Dirmeyer, P. A. (2020). Reconciling the disagreement between observed and simulated temperature responses to deforestation. *Nature Communications*, 11(1), 202. <https://doi.org/10.1038/s41467-019-14017-0>
- Davidson, E. A., de Araújo, A. C., Artaxo, P., Balch, J. K., Brown, I. F., C. Bustamante, M. M., et al. (2012). The Amazon basin in transition. *Nature*, 481(7381), 321–328. <https://doi.org/10.1038/nature10717>
- Liu, Y., Guo, W. D., Huang, H. L., Ge, J., & Qiu, B. (2021). Estimating global aerodynamic parameters in 1982–2017 using remote-sensing data and a turbulent transfer model. *Remote Sensing of Environment*, 260, 112428. <https://doi.org/10.1016/j.rse.2021.112428>
- Malhi, Y., Roberts, J. T., Betts, R. A., Killeen, T. J., Li, W., & Nobre, C. A. (2008). Climate change, deforestation, and the fate of the Amazon. *Science*, 319(5860), 169–172. <https://doi.org/10.1126/science.1146961>

- Nobre, C., Encalada, A., Anderson, E., & Neves, E. G. (2021). Science panel for the Amazon: Amazon Assessment Report 2021: Executive summary.
- Restrepo-Coupe, N., O'Donnell Christoffersen, B., Longo, M., Alves, L. F., Campos, K. S., da Araujo, A. C., et al. (2023). Asymmetric response of Amazon forest water and energy fluxes to wet and dry hydrological extremes reveals onset of a local drought-induced tipping point. *Global Change Biology*, 29(21), 6077–6092. <https://doi.org/10.1111/gcb.16933>
- Reygadas, Y., Spera, S. A., & Salisbury, D. S. (2023). Effects of deforestation and forest degradation on ecosystem service indicators across the Southwestern Amazon. *Ecological Indicators*, 147, 109996. <https://doi.org/10.1016/j.ecolind.2023.109996>
- Sierra, J. P., Junquas, C., Espinoza, J. C., Segura, H., Condom, T., Andrade, M., et al. (2021). Deforestation impacts on Amazon-Andes hydroclimatic connectivity. *Climate Dynamics*, 58(9–10), 2609–2636. <https://doi.org/10.1007/s00382-021-06025-y>
- Yang, H., Ciais, P., Wigneron, J.-P., Chave, J., Cartus, O., Chen, X., et al. (2022). Climatic and biotic factors influencing regional declines and recovery of tropical forest biomass from the 2015/16 El Niño. *Proceedings of the National Academy of Sciences of the United States of America*, 119(26), e2101388119. <https://doi.org/10.1073/pnas.2101388119>
- Zeng, Z. Z., Piao, S. L., Li, L. Z. X., Wang, T., Ciais, P., Lian, X., et al. (2018). Impact of Earth greening on the terrestrial water cycle. *Journal of Climate*, 31(7), 2633–2650. <https://doi.org/10.1175/JCLI-D-17-0236.1>